Measurement Method for Simple Determination of Sinusoidal Large Signal Losses in Inductive Components

Peter Zacharias[1], Alejandro Aganza-Torres[2]
[1]University of Kassel, Wilhelmshoeher Allee 71, D-34131 Kassel, Germany, Tel.: +49 / 561 – 804 6344 Fax: +49 / 561 – 804 6351. E-Mail: peter.zacharias@uni-kassel.de.com
[2]Autonomous University of San Luis Potosi, Multidisciplinary Academic Unit Middle Zone, Rioverde-San Ciro Road Km. 4, 79617, Rioverde, Mexico, e-mail: alejandro.aganza@uaslp.mx

Keywords

«Magnetic device», «Magnet loss», «Passive component», «Permeability», «Standardization

Abstract

In this work, a resonance-based losses measurement method is shown suitable for the power dissipation measurement of small and large inductive components under sinusoidal test voltage. In a resonance-based measurement method, the magnetic losses of inductive devices are transformed to the measurement of electrical RMS magnitudes through the device under test. The sinusoidal shape of the test voltage is therefore inherently guaranteed in the measurement procedure.

Introduction

Magnetic components are largely responsible for the weight and volume of power electronic converters. The decisive factor in their use is that certain limit temperatures are not exceeded. This enables long service lives to be achieved. In addition to the saturation of the core, losses during operation thus represent important limits that must not be exceeded. A distinction must be made between winding and core losses, because of the nonlinear properties and the sometimes very high quality factors that can be achieved with ferromagnetic core materials, reliable measurement of losses in cores is difficult. Data on losses in core materials are given mainly for sinusoidal excitation in the small-signal range on small toroidal cores [1]. These values cannot be applied to arbitrary large cores and non-sinusoidal quantities for several reasons. One reason is the non-constant magnetic flux density for many core shapes. Because of the nonlinearity of the relationships, the superposition principle cannot be applied to the individual sections. Then other ways have to be searched [2, 3, 4]. If it is possible to provide sinusoidal voltages with sufficient quality or low THD, electrical measurement methods can be used which are characterized by very short measurement times [1, 6]. For non-sinusoidal voltages at the inductor, only calorimetric measurement methods [2, 7, 8] are reasonably applicable. To a large extent, one can dispense with precision measurement equipment if, instead of phase angle measurement, bridge balancing is used [8], as described in the following article. Electrical measurement methods have the great advantage that they provide results several orders of magnitude faster than calorimetric measurement methods. The paper presents a resonance-based measurement method to map losses of an inductive device to the relatively simple measurement of RMS voltages. Alternatives to approximately separate winding losses from total losses are also shown.

Parallel resonance as the basic idea of the measurement method

If you connect a capacitance in parallel to an inductance, you get a parallel resonant circuit. At its resonant frequency, the impedance becomes maximum and the imaginary part of the impedance becomes zero. Only the power to cover the losses of the resistive component is supplied to the terminals of the resonant circuit. The reactive power, which is usually much higher, is exchanged between the inductive component and the capacitance. Even with non-sinusoidal current, harmonics are strongly suppressed by the integrating behavior of the capacitance in the voltage. The sinusoidal shape of the voltage, which is an important secondary condition for the comparability of the measurement conditions, is thus maintained over a wide voltage and frequency range. Due to the clearly dominating fundamental oscillation at the resonance frequency, the classical methods of alternating current calculation can be used for loss determination with good justification. Fig. 1a shows the principle of the measurement. E_1 represents a voltage source with variable frequency and sinusoidal voltage. This source also has to supply the total losses in the measurement circuit. The resonant capacitor C_1 is in parallel

with the DUT (Device Under Test) and supplies the required reactive power for it. The resistor R_1, like the capacitor C_1, must be selected as precision components, as the measured losses and inductance values of the DUT are determined in reference to these components. At resonant frequency f_{res}, the phase shift between voltages V_1 and V_2 is zero. This is easy to detect. In the resonance case (Fig. 1b), the complexity of the circuit is reduced if all losses are lumped to a resistor R_{loss}.

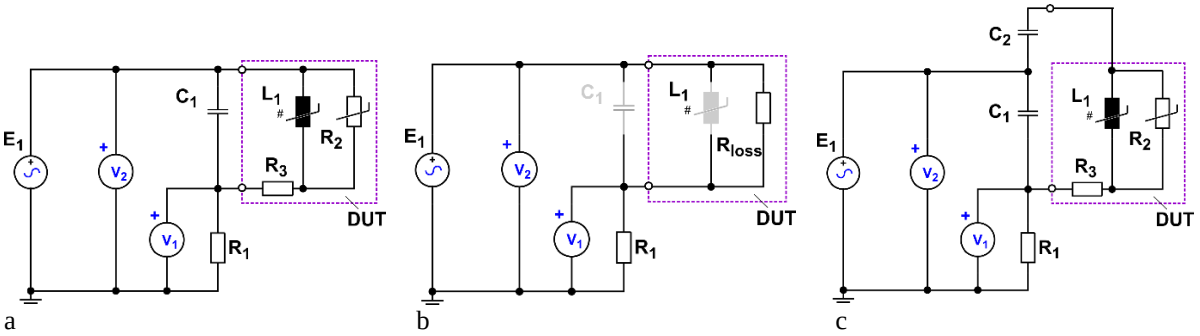

Fig. 1: Principle structure for determining the losses of an inductive component in the large signal range: a basic circuit, b remaining structure in the resonance case, c - extension of the circuit to achieve higher voltages at the DUT.

Thus, the resistance R_{loss} can be determined from the known quantities.

$$R_{loss} = \left(\frac{U_2}{U_1} - 1 \right) R_1 \quad \text{therefore:} \quad P_{loss} = \frac{(U_2 - U_1)^2}{R_{loss}} = \frac{(U_2 - U_1) U_1}{R_1}$$

In the resonance case, equal amounts of magnetic energy are exchanged with amounts of electrical energy. This results in the effective inductance L_{eff} via the formula

$$L_{eff} = \frac{1}{(2\pi f_{res})^2 \cdot C_1}$$

The modification in Fig. 1c allows the test voltage at the DUT to be increased. The calculations of P_{loss} and L_{eff} must then be adjusted accordingly.

Realization of a measurement setup according to the described principle

Fig. 2 shows how such a measurement setup can be realized with simple means. Fig. 2a shows an overview of the interaction of the individual components. Fig. 2b shows the laboratory setup. In order to be able to record series of measurements at the same frequency, the capacitance C_1 was designed to be variable via switchable capacitance decades. The capacitances must have low tolerances and low losses, since they serve as reference elements. The sinusoidal voltage is generated with an adjustable frequency generator and amplified from a level of 1Vrms to 100Vrms with a high-fidelity power amplifier. The nominal power of the amplifier is 100W. It should be noted that this power only covers the power dissipation requirements of the DUT and R_1. The reactive power in the resonant circuit can be many times higher. The capacitors and switches must therefore be designed for the possible currents and voltages at resonance. In the case shown, this is 6A and 100V as a continuous load.

The oscilloscope is used in the measurement setup to determine the resonance case or resonance frequency and to measure the voltages V_1 and V_2. The measurements are then further used for evaluation according to the presented algorithms. The frequency range of the power amplifier is 10kHz - 12MHz. Currently, based on this basic design, a measurement setup is being implemented with air rotary capacitors in the range of 25pF - 1.5nF, mica capacitors up to 100nF and film capacitors up to 10x10uF. This is to cover the widest possible range of measurement tasks of interest. With the resistor R_1 it is possible to switch between different measuring ranges for the power dissipation. Since current flows continuously during adjustment and measurement to cover the losses in the parallel resonant circuit, R_1 must be able to dissipate this power loss. This means that low inductance and easy to cool footprints are considered for R_1. Both the leads and the junctions must be suitable for the relatively large currents flowing through the resistor.

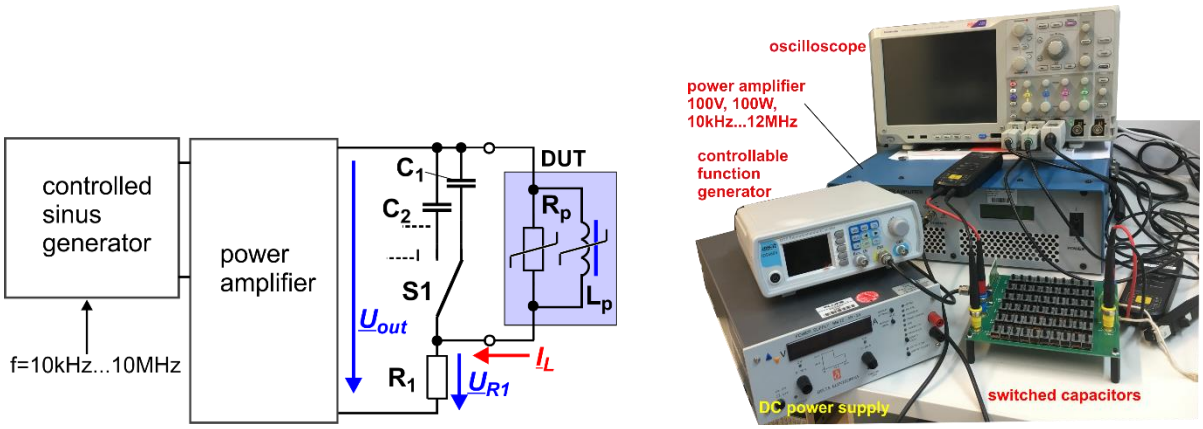

Fig. 2: Set-up of the laboratory test bench for determination of losses in inductive components: a - principle set-up, b - laboratory realization with devices and manually switched capacitors.

Separation of winding and core losses

Even simple inductive components have a considerable complexity. Fig. 3 shows an electrical equivalent circuit for a winding with a ferromagnetic core. Due to the induced electric field, the magnetic field of the winding leads to losses via dielectric and galvanic currents in the core. These are represented in the model by the parallel resistance Rcore(f,U). For both, it can be assumed that they are dependent on both the induced voltage and the frequency.

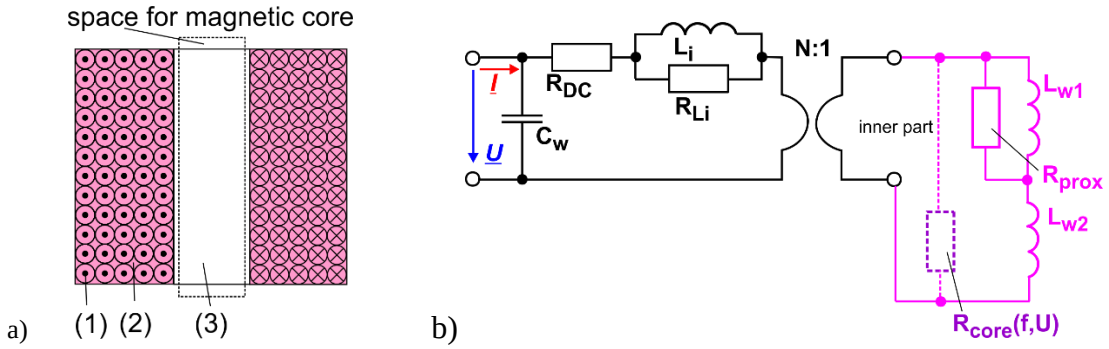

Fig. 3: Modeling of a winding on a core: a) drawing: (1) winding wire with skin effect, (2) winding with proximity effect and (3) space filled with magnetic field, which may be filled with core material; b) equivalent circuit derived from a) with consideration of the individual loss components.

Through the transformer with the number of turns N, the voltage U applied to the terminals of the component becomes the voltage induced on a turn in the core. The winding without a core has a DC resistance R_{DC} and an intrinsic inductance, which is formed by the internal inductance L_i, the winding inductance L_{w1}, which is formed by the linked magnetic field of the winding penetrated by the stray field, and the inductance L_{w2}, which is formed by the linked magnetic flux in the space not filled by magnetic materials. The transformation ratio of the intrinsic ideal transformer transforms these quantities to the terminals of the device (Fig. 4). The internal inductance L_i leads to losses due to eddy currents. At the same time, field displacement takes place, resulting in a reduction of the internal inductance and an increase of the effective resistance. If core material is added, the equivalent circuit for the entire device is obtained. This is in accordance with the rules of structural analysis for magnetic circuits. Since the magnetic field of the component enters the winding material, it causes eddy current losses there. Because of the transformer coupling of these losses, a parallel resistor R_{prox} is physically appropriate as their representative.
The series connection of L_{w1} and L_{w2} also corresponds to the physical conditions. If a core material is inserted, the resulting losses can be represented by a resistance R_{core} parallel to L_{w2}. This is not only dependent on the frequency but also on the voltage. This equivalent circuit reflects the basic physical relationships and approximately the quantitative relationships. With a determination of the properties of the winding without core, the winding losses can thus be determined approximately for a balancing calculation.

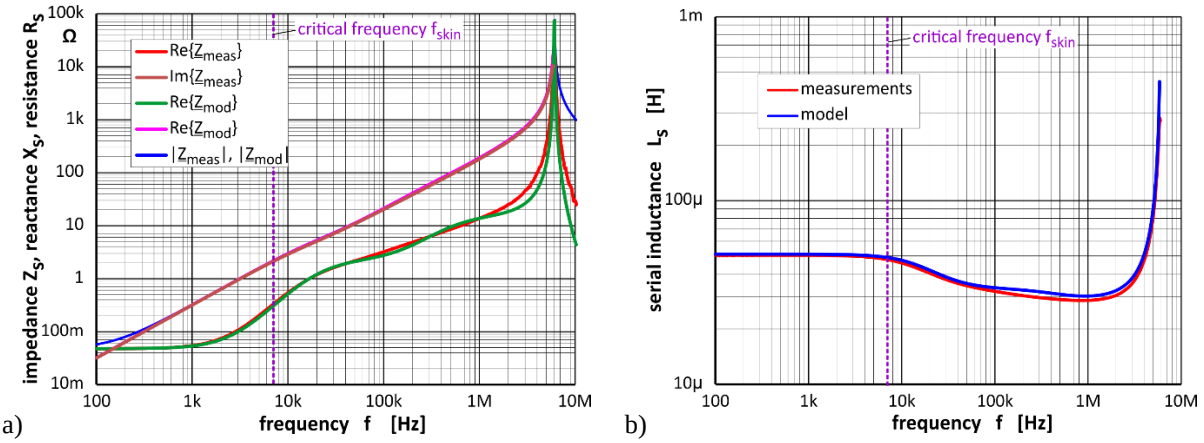

Fig. 4: Measured and calculated impedance and real components of the impedance Z_s (a); Measured and calculated course of the inductive part of the impedance (DUT: solenoid coil, d_{Al} = 2mm, 38x12x18mm, N = 60; model parameters related to the terminals: R_{DC} = 477mOhm, L_i =4.5µH, R_{Li} = 13Ohm; L_{w1}=18µH, R_{prox} = 2.2Ohm, L_{w2} = 28.6µH, R_{core} = ∞, C_w = 24pF).

Fig. 4 compares the measurement results for a short coreless cylindrical coil (solenoid coil; D x d x l = 38mm x 10mm x 18mm) made of 2mm thick aluminium wire with the calculations for a model according to Fig. 3b. It is clear that the increase in losses (represented by the measured real component of the impedance) already start well below the critical frequency f_{skin}. Here f_{skin} is the frequency at which the formal skin thickness of the current is equal to the radius of the wire. Above this frequency, one observes a decrease in the effective inductance L_s=Im{Z_s}/(2πf). Physically, this is due to the onset of displacement of the magnetic field not only from the winding wire (skin effect) but also from the interlinked region of the winding. The apparent increase of the inductance at approx. 6MHz is caused by the parallel resonance of the effective inductance with the winding capacitance C_w. This leads to an apparent increase of the inductance by the calculation rule.
Actually, the field displacement leads to a loss increase by a factor of ~$f^{0.5}$. A component with such properties does not exist as a basic element in electrical engineering. Although it can be simulated by an LR cascade arrangement. Consequently, the example shown is only an approximation. The found agreement of the model data with the measured data is however already quite appropriate in the frequency range <f_{res}, which is interesting for the application of the component. The parameter found for L_i represents both the skin effect in the wire and the shielding effect between the layers in the proximity effect. It is therefore significantly larger than the actual internal inductance of the wire used (112nH).

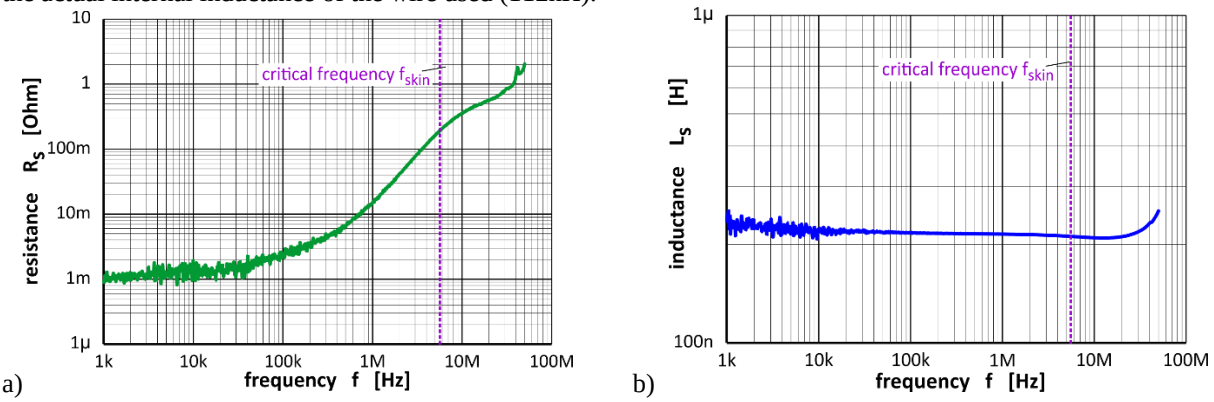

Fig. 5: Measurement results for the impedance components of a coil without core according to Fig. 6 with plotted critical frequency for the skin effect: a) serial resistance Rs; b) serial inductance Ls (fitted model values: R_{DC} = 1mOhm, L_i = 18nH; R_{Li} = 25Ohm; L_{w1}=10nH, R_{prox} = 0.22Ohm, L_{w2} = 190nH, R_{core} = ∞, C_w = 9pF).

The extent of the proximity effect depends on the structure of the winding and the associated stray field in the winding. In Fig. 5, the measured frequency-dependent curves of the real and imaginary parts of the impedance of a single-layer cylindrical coil are shown in Fig. 6 for comparison with Fig. 4. In this case, the magnetic field lines are drawn comparatively long. For this reason, the magnetic field strength tends to be lower than for a solenoid coil. This is associated with lower eddy current losses in the conductor material. In addition, the structure shown uses stranded copper wire 4x (1575 x 0.071mm) as the conductor material. This leads to a much higher critical skin frequency than in Fig. 5. It can also be seen here that the proximity losses become dominant at frequencies much lower than the critical skin frequency.

The approach of taking the losses in the winding material into account is that, in addition to the described measurement of the losses with nearly sinusoidal voltage waveforms, the resulting winding losses are calculated with the help of the model. The parameterization of a model for a winding without a core then allows the expected losses in the entire inductive component to be determined by combining it with a (partially linearized) loss model of the core $R_{core}(U, f)$ in a simulation.

Measurement example

Fig. 6 shows some first measurement results with the previously described principle. Fig. 6a shows the mechanical design of the DUT. On a UR64 core there are 8 x 3 windings of HF stranded wire 1575 x 0.071mm. This keeps the loss components of the winding very low by design. All partial windings are connected in parallel. This "forces" the flux into the core. For the measurement results shown, no air gap was inserted between the core halves. Measurement results for this no air gap condition and for parallel premagnetization will be reported in the main paper. As the UR64 core has a hole for mounting, this is used for a flexible line for a premagnetization current Id to be supplied. This premagnetization current is oriented parallel to the alternating magnetic field of the coils. This means that the main magnetic field and the field for premagnetization are perpendicular to each other. This is called orthogonal premagnetization, and in this case the fields add geometrically. When the result of this superposition enters the saturation region, small and large signal inductance of the main coil change. One of the questions to be investigated was to what extent the losses or the quality factor Q also change. Figs. 6b and 6c show some results of the evaluation of the measurements.

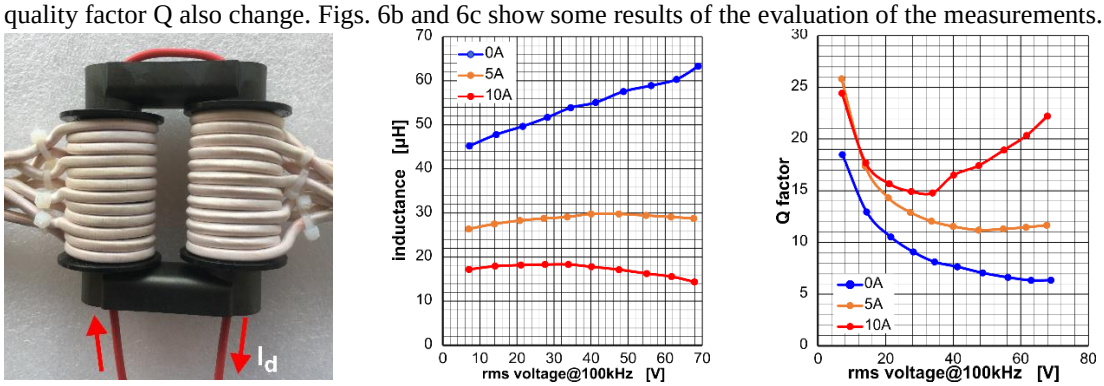

a b c

Fig. 6: Measurement results for a Ferroxcube UR64 ferrite core orthogonally premagnetized with a current Id. a- Mechanical structure; b - Effective inductance as a function of RMS voltage and premagnetization current Id and c - Quality factor Q as a function of RMS voltage and premagnetization current Id.

The premagnetization obviously has a significant influence on the inductance of the winding and on the quality factor Q. As expected, the inductance decreases with increasing premagnetization current. An ever increasing current Id means that an ever increasing proportion of the core cross-section around the premagnetization wire becomes saturated and is no longer available for the "concentration" of the magnetic field. This tendency becomes even more pronounced at higher voltages.

If only the losses are considered, after a mathematical subtraction of the winding losses, the results can be plotted in a double logarithmic representation. Then Fig. 7a is obtained. Each of the measurement series is approximated by a power function according to the Steinmetz formula. It can be seen that each of the measurement series yields almost straight lines at this scale. This impression is also confirmed when the measured values are plotted relative to the power function for I_d = 0A (Fig. 7b). Nevertheless, it can be observed that in the lower voltage range the relative deviations are larger than in the upper voltage range. These observations can be used in conjunction with the other measurements for further conclusions. One advantage of the method is that the oscillating circuit capacitor with its high Q factor supports the voltage at the inductive component intrinsically. This makes measurement results easily comparable with each other. Moreover, the change at each measurement point is made instantly, which in comparison with calorimetric measurements, are much faster and less dependable of environmental conditions of the operation of the DUT.

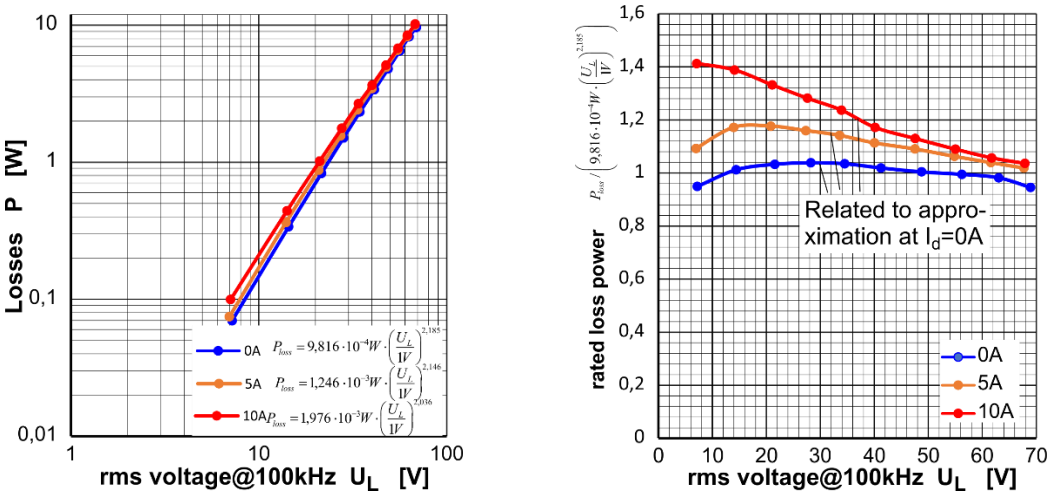

a b

Fig. 7: Measured power losses as a function of RMS voltage and bias current I_d: a - determined core losses; b - relative deviation of measured values compared to Steinmetz approximation at I_d=0

Design of a measurement setup for a wide range of values in general laboratory applications

In large-signal measurements, one usually has relatively high RMS values for voltages and currents. This must be taken into account when selecting and constructing a measuring arrangement. Fig. 8 shows a revised measurement arrangement according to the presented principle. Here, too, the 100W broadband amplifier has to cover only the losses in the DUT and the measurement resistors. In addition to these losses, there are very small contributions from the capacitive elements. These must therefore be selected with the highest possible Q values. In the range up to 1100pF, variable capacitors with air insulation are used. These show very low losses compared to ceramic or film capacitors. To maximize the stability of the capacitance of these capacitors, they are operated in a hermetically sealed room with dried air. Fig. 8b shows the structure of the two switchable variable capacitors in the open state. The capacitance value of each of these capacitors is set manually by means of a fine gear connected to a scale for displaying the current capacitance value.

Further capacitance values can be set by means of changeover switches with mica capacitors up to the range of 100nF. The set capacitance values are required for the evaluation of the measurement results according to the procedure described above. Above 100nF, film capacitors with selected low series loss resistances are used. The frequency-dependent permissible values of current and voltage for the capacitors set limits for measurement ranges. One must not forget that at frequencies >100kHz high reactive powers and thus high currents are already reached even with small capacitance values. For the time of the measurement these should not cause any noticeable heating. Then the loss resistances of the capacitors measured in the small signal range can also be considered in the power loss balance.

The entire setup shown in Fig. 8 is intended for manual operation. By using capacitance values in decades, it is not possible to set an "exact" value for the capacitance due to the discretization. Even considering the possibility of setting fine capacitance values with the variable capacitors, such a goal would be limited by the tolerances of the capacitance values. The individual measurement of each capacitor before installation in the measuring device, mitigates this problem. The sometimes high currents also flow through the switches, which must also be suitable for this purpose. It is therefore advisable to start with small voltages for large-signal measurements and then increase them step by step. Then it is also possible to switch over without problems during the measurement. Typically, the effective inductance then changes somewhat and the resonance ($\Delta\varphi = 0$) must always be readjusted at the new test voltage by adjusting the resonance capacitance value.

The measuring range switching is done with low inductive precision resistors. Since these resistors generate up to 50W of heat, they are mounted on a heat sink which is forced cooled by fans Fig. 8a.

a 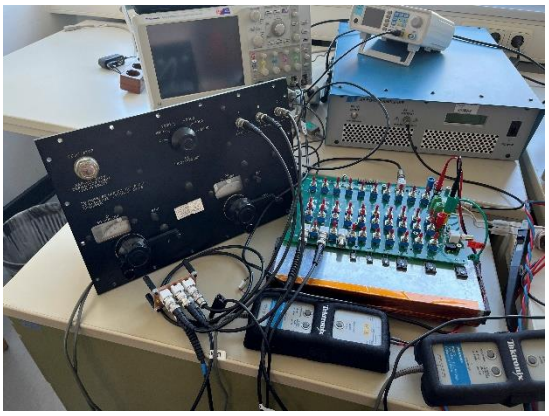 b 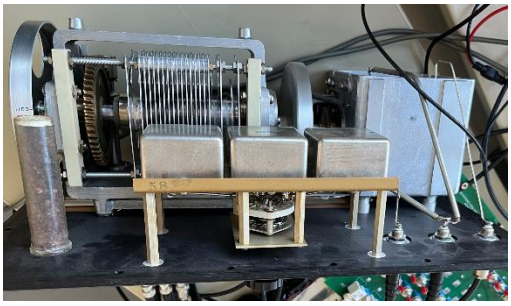

Fig. 8: Structure of the described measuring arrangement before covered: a) Circuit board with the switched and cooled resistors and switched capacitors for the measurement, b) Illustration of 2 variable capacitors (10pF...210pF and 50pF...1100pF) with high Q which is extended to 6100pF with 3 mica caps (1000pF and 2x 2000pF) for the higher frequency range.

Finally, Fig. 9 shows the setting and measuring ranges resulting from the selected setup. To measure a specific core, a suitable number of turns is applied to it. Suitable here means that the measurements of interest can be carried out in the frequency and capacitance ranges available in the setup in Fig. 8.

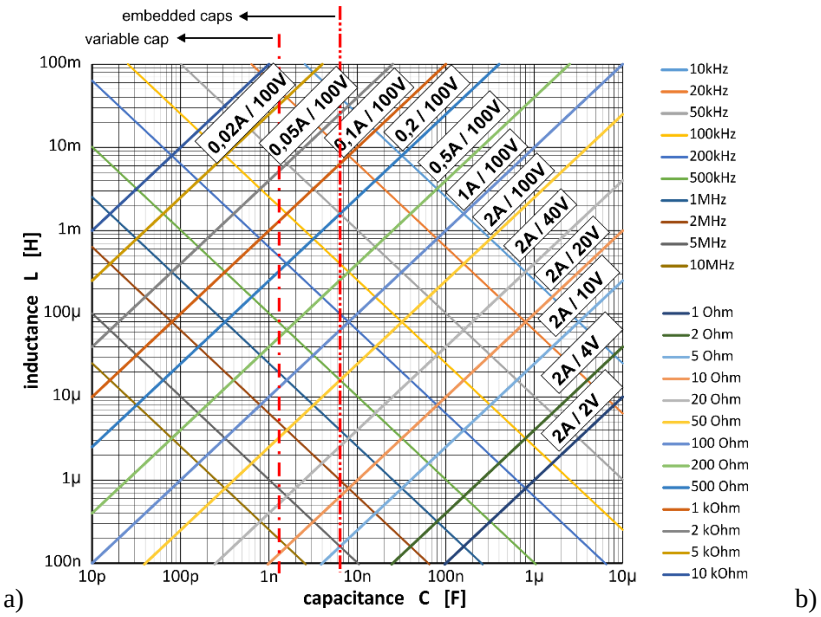

a) b)

Fig. 9: Relationship between inductance, capacitance, characteristic impedance and measuring frequency for the measuring device (current and voltage values are only orientations here)

Conclusions

In this paper, a resonance-based measurement method is suitable for determining the losses of practically arbitrary cores shapes under sinusoidal voltage loading. The original problem of balancing active and reactive power components, which is usually subject to considerable measurement uncertainties, especially for high-quality inductive components, is transformed into a problem where inherent averaging is performed. Thus, effects of individual measurement errors are strongly suppressed. It is possible to measure both the energetically effective large-signal inductance and the large-signal losses up to relatively high magnetic field strengths. Due to the exclusive use of electrical quantities, the measurement process takes only a very short time compared to the self-heating of the inductive components using the calorimetric measurement method. Application possibilities

and statements of the measuring method flexibility are shown on the example for different types of pre-magnetization. A setup for measurement in manual mode was presented. Next steps are to automate this setup.

References

[1] International Electrotechnical Comission, “IEC 62044-1:2002. Cores made of soft magnetic materials - Measuring methods - Part 1: Generic specification ”, May 2002.

[2] C. Xiao, G. Chen and W. G. H. Odendaal, "Overview of Power Loss Measurement Techniques in Power Electronics Systems," in IEEE Transactions on Industry Applications, vol. 43, no. 3, pp. 657-664, May-june 2007, doi: 10.1109/TIA.2007.895730.

[3] Lopez-Lopez, J.; Fernandez, C.; Barrado, A; Zumel, P. Comparison of Different Large Signal Measurement Setups for High Frequency Inductors. Electronics 2021, 10, 691. https://doi.org/10.3390/ electronics10060691

[4] Zhang, Yu & Alatawneh, Natheer & Cheng, Ming-Cheng & Pillay, P.. (2009). Magnetic core losses measurement instrumentations and a dynamic hysteresis loss model. 10.1109/EPEC.2009.5420918.

[5] F. Dong Tan, Jeff L. Vollin, and Slobodan M. Cuk : “A Practical Approach for Magnetic Core-Loss Characterization”, IEEE TRANSACTIONS ON POWER ELECTRONICS, VOL. 10, NO. 2. MARCH 1995.

[6] ZES Zimmer, “Measurement of magnetic characteristics of transformer-cores and coil materials. Application Note 103 (Rev. 2.0)”, https://www.zes.com/en/Service/Downloads/Documents/Application-Notes/103-Measurement-of-the-magnetic-properties-of-transformers-and-coil-cores, Accessed: May 2022.

[7] F. Zámborszky, D. Tóth, Z. Palánki and E. Csizmadia, "Electrical and Calorimetric Power Loss Measurements of Practically Ideal Soft Magnetic Cores," in *IEEE Transactions on Magnetics*, vol. 50, no. 4, pp. 1-4, April 2014, Art no. 6300604, doi: 10.1109/TMAG.2013.2286700.

[8] P. Zacharias: Magnetische Bauelemente. Springer-Nature 2020. ISBN 978-3-658-24741-6, https://doi.org/10.1007/978-3-658-24742-3